

# 1 **Simulate Before Sending: 2 Rethinking Transport in Datacenter Networks**

3 **Dan Straussman** 

4 Technion, Israel

5 **Isaac Keslassy**   

6 Technion, Israel

7 UC Berkeley, USA

8 **Alexander Shpiner** 

9 Nvidia

10 **Liran Liss** 

11 Nvidia

---

## 12 **Abstract**

13 Existing transport protocols in commodity datacenter networks struggle to provide low collective  
14 completion times (CCTs) to AI training collectives, as packet losses and retransmissions significantly  
15 degrade performance.

16 We propose **DCSIM**, an efficient transport that achieves low CCTs and *practically lossless*  
17 performance with commodity switches. In **DCSIM**, each packet first employs a small simulation  
18 probe to traverse the network and explore congestion along a candidate path. Only packets whose  
19 simulation probes succeed are then transmitted, expecting to succeed as well. Evaluations confirm  
20 that **DCSIM** achieves faster CCTs than existing schemes, with small queues and virtually zero packet  
21 loss. Finally, **DCSIM** also excels in adverse conditions, including oversubscribed topologies.

22 **2012 ACM Subject Classification** Networks → Data center networks; Networks → Transport  
23 protocols

24 **Keywords and phrases** Datacenter networks, transport protocols, AI training, lossless networks

25 **Digital Object Identifier** 10.4230/OASIcs.NINeS.2026.19

26 **Funding Isaac Keslassy:** This work was partly supported by the Louis and Miriam Benjamin Chair  
27 in Computer-Communication Networks.

## 28 **1 Introduction**

29 Datacenters are increasingly designed for AI training. Large companies such as Google, Meta,  
30 OpenAI, AWS and Microsoft are planning to invest hundreds of billions of dollars to support  
31 AI workloads in their cloud infrastructure [35, 44, 7, 43, 20, 2, 45].

32 Unfortunately, due to their computation/communication cycles, AI training applications  
33 are very bursty, and can incur significant *packet drop rates* in lossy datacenter networks [47,  
34 13, 46]. In addition, while AI training traffic patterns used to be more symmetric and  
35 predictable, recent mixture-of-experts (MoE) models exhibit unpredictable patterns that  
36 worsen packet drops [33, 32, 21, 22, 13, 30, 51].

37 These packet drops harm AI training performance in two ways. First, they cause stragglers  
38 due to packet retransmissions, and therefore increase collective completion times (CCTs),  
39 i.e., the time for the last packet to complete in a collective communication algorithm like  
40 Ring All-Reduce or All-to-All [47, 34]. Second, packet losses can also increase the tail  
41 latency of RDMA, a common building block for AI training applications designed for lossless  
42 networks [36, 16, 38, 52, 13, 27].



© Dan Straussman, Isaac Keslassy, Alexander Shpiner and Liran Liss;  
licensed under Creative Commons License CC-BY 4.0

1st New Ideas in Networked Systems (NINeS 2026).

Editors: Katerina J. Argyraki and Aurojit Panda; Article No. 19; pp. 19:1–19:22

OpenAccess Series in Informatics

 **OASIcs** Schloss Dagstuhl – Leibniz-Zentrum für Informatik, Dagstuhl Publishing, Germany

43     *Thus, there is a need to design transports that lower CCTs by making commodity lossy*  
 44 *networks practically lossless.* To fully exploit the network capacity, many solutions use  
 45 per-packet load balancing, including oblivious packet spraying, such as in Alibaba Stellar [12,  
 46 59, 18, 34]; adaptive packet spraying, such as in STrack, REPS, and the Ultra Ethernet  
 47 Consortium specification [25, 9, 56, 47]; and adaptive routing, such as in NVIDIA’s Spectrum-  
 48 X [1, 39, 57, 41, 50]. These solutions use several reliability mechanisms to handle losses, e.g.,  
 49 NACK-based and selective-repeat mechanisms in extended RoCE-based protocols [16, 38, 52],  
 50 or packet trimming [8, 42, 56, 27]. However, these schemes can experience poor performance  
 51 when scaling [36, 27, 27]. Another approach, adopted by pHost [14] and dcPIM [10], is to  
 52 rely on a matching algorithm where receivers grant tokens to senders. This approach is  
 53 promising because it avoids losses due to receiver oversubscription, but it also lacks visibility  
 54 into the network and is therefore vulnerable to oversubscribed networks and link failures.

55     Additional schemes show great potential for avoiding losses, but require non-commodity  
 56 hardware. Rateless erasure coding can mask losses but needs specialized NICs to be imple-  
 57 mented at high rates [24, 36]. ExpressPass introduces a receiver-driven credit-based scheme  
 58 that avoids losses, but it relies on switch modifications, e.g., to ensure symmetric paths, and  
 59 cannot handle multi-path and link failures [11]. Harmony offers another promising direction:  
 60 using *reservations* [3]. Harmony uses per-flow fixed-bandwidth reservations to eliminate  
 61 congestion-related drops while achieving high utilization. Unfortunately, it also needs spe-  
 62 cialized switches to participate in the reservation process, and struggles with low-rate and  
 63 variable-rate flows that do not match the fixed reservation rates.

64     To achieve our goal of a practically-lossless transport running in a lossy network with  
 65 commodity hardware, we want to use reservations and solve two significant challenges that  
 66 currently limit their effectiveness. First, the reservations need to be more flexible, with  
 67 *per-packet reservations* that allow the flow path to change upon congestion. Second, they  
 68 should be made with *commodity switches* and thus be implementable at any datacenter.

69     We present DCSIM, an effectively lossless transport mechanism that can achieve low CCT  
 70 for AI training with commodity switches, while being resilient to adverse network conditions.  
 71 It relies on two core ideas to address the reservation challenges. The first one is a conceptual  
 72 shift. Assume we had a *shadow simulation network* that could run at exactly 1/100th the  
 73 rate of our real network, with load-balanced SIM (simulation) packets that are also 100  
 74 times smaller than our real-network DATA packets. Then if each shadow SIM was sent in  
 75 the shadow network at the same time as its corresponding DATA in the real network, it  
 76 would also experience the same propagation, transmission and queueing delays. We can  
 77 exploit this shadow network as follows. As source hosts are about to send DATAS, their  
 78 corresponding SIMs are sent instead in the shadow network and load-balanced across random  
 79 paths. Some may be dropped at some congested buffer of size  $B$  that is already full of  $B$   
 80 other SIMs. Others will reach their destination as their buffers were less congested, and an  
 81 acknowledgment will get back to the source host. Then, a fixed time later, we only send the  
 82 DATAS that correspond to SIMs that arrived, through the exact same path. We are intuitively  
 83 guaranteed that the DATAS will also arrive: if a DATA is blocked at some buffer by  $B$  DATAS,  
 84 it means that its SIM would also have been blocked by their corresponding  $B$  SIMs, which  
 85 did not happen. As for any DATAS with a blocked SIM, we simply send a new SIM to probe  
 86 a new random path.

87     The above concept is appealing, but not practical. The second key idea is to *approximate*  
 88 *the shadow SIM network by using dedicated buffers* for SIMs and DATAS. Many commodity  
 89 switches support partitioning their buffers based on different traffic classes. Now SIMs and  
 90 DATAS coexist in the same network and share its capacity. Each SIM effectively implements

91 reservation on a given path for a place in the DATA buffers that will be used when sending  
 92 a DATA some fixed time later. Intuitively, DCSIM trades off a small portion of the network  
 93 capacity to ensure a practically lossless network, and thus avoid a more significant loss of  
 94 capacity due to DATA losses.

95 In evaluations, DCSIM consistently outperforms existing schemes under several collective  
 96 workloads. It exhibits better CCTs, higher utilization, *no packet drops*, minimal switch  
 97 queueing, and negligible reordering. It shines even more under adverse conditions, such as a  
 98 core-switch oversubscription, as it keeps low CCTs and zero drops while other algorithms  
 99 suffer from high loss rates.

100 **Contributions.** In summary, we make the following contributions.

- 101 ■ We introduce the new conceptual framework of simulating paths before sending packets.
- 102 ■ We design DCSIM to follow this framework while being fully deployable on commodity  
 103 datacenter networks.
- 104 ■ We show that DCSIM achieves low CCTs using a *practically lossless transport*.
- 105 ■ We show that DCSIM maintains high performance under challenging scenarios, including  
 106 oversubscribed topologies and small switch queues.

107 The DCSIM source code is available online [53].

## 108 2 DCSIM Algorithm

### 109 2.1 Design goals

110 We design DCSIM to achieve the following goals:

111 **1. No loss.** DCSIM should have a near-zero loss probability, despite running in a lossy  
 112 commodity network. With zero data loss, there is no need to retransmit data, and forward  
 113 progress is guaranteed.

114 **2. Low queueing.** In modern datacenter networks, “queueing delays and buffer overflow  
 115 are the root cause of unpredictability” [3]. DCSIM should offer a low-queueing solution that  
 116 enables flexibility to changing patterns.

117 **3. Per-packet load-balancing.** DCSIM should be able to offer per-packet load-balancing  
 118 to fully utilize the network capacity and address challenging conditions such as failed or  
 119 congested links.

120 **4. Several collectives.** DCSIM should be able to handle several concurrent collectives with  
 121 many flows simultaneously fighting for a chunk of network capacity.

122 **5. Commodity switches.** DCSIM should not rely on any non-readily available switch feature.

### 123 2.2 DCSIM overview

124 DCSIM relies on a packet transmission approach that operates in two distinct phases for each  
 125 DATA packet from source  $S$  to destination  $D$ :

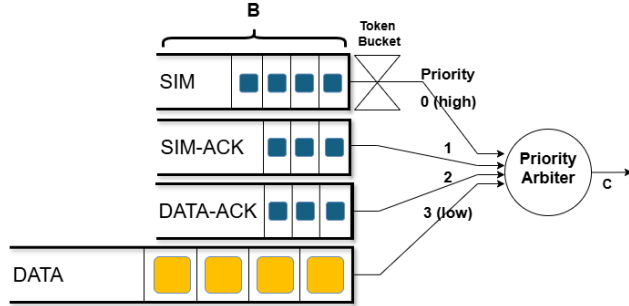


Figure 1 DCSIM queueing mechanism

126 **1. A simulation phase,** during which a small SIM (simulation) packet is transmitted  
 127 through a random path from  $S$  to  $D$ . At each commodity switch along the path, SIMs are  
 128 queued in a SIM queue, distinct from the DATA queue for DATAs. The SIM queue has strict  
 129 priority over the DATA queue, but its service is rate-limited in a way that allows SIMs and  
 130 DATAs to leave in an alternating sequence and fully occupy the line, thus reaching an ideal  
 131 utilization. Any SIM that arrives at the SIM buffer enters the queue if there is space, and is  
 132 dropped otherwise. Once a SIM reaches  $D$ ,  $D$  sends back a SIM-ACK to  $S$ .

133 **2. A data phase,** during which the DATAs are sent along the same path previously traversed  
 134 by their counterpart SIMs. To reduce reordering, DCSIM associates to each successful SIM  
 135 the first DATA waiting in the queue. This DATA is then sent  $RTT_{\max}$  time after the SIM  
 136 was sent, where  $RTT_{\max}$  is a fixed datacenter-wide bound on the SIM RTT (cf. § 2.5). Let's  
 137 focus on a specific  $SIM_0$  and its corresponding  $DATA_0$ . Assume that  $SIM_0$  competes with  
 138 other SIMs for switch buffer occupancy, and manages to get through. Then when  $DATA_0$   
 139 later competes with other DATAs, we expect it to have no more competitors than  $SIM_0$ , and  
 140 in fact it may have fewer competitors if some SIMs got dropped in later switches. We thus  
 141 expect  $DATA_0$  to enter the switch buffers and later reach its destination without any drop.  
 142 That is, *we expect the DATAs not to experience any drop, and in fact to experience slightly*  
 143 *less congestion than their corresponding SIMs.*

### 144 2.3 Switch queueing mechanism

145 **Overview.** Fig. 1 illustrates the DCSIM queueing mechanism, which is implemented at  
 146 each switch output and at hosts. It consists of a priority arbiter that implements a strict  
 147 priority without preemption between four queues, dedicated to the four data types in this  
 148 paper: (i) SIMs, (ii) SIM-ACKs, (iii) DATA-ACKs and (iv) DATAs. SIM-ACKs and DATA-ACKs  
 149 acknowledge reception of SIMs and DATAs, respectively. SIMs (serviced at the highest priority)  
 150 are rate-limited using a token bucket.

151 The SIMs, SIM-ACKs, and DATA-ACKs are small packets of size  $\ell$  (e.g.,  $\ell = 64$  bytes),  
 152 and their queues are stored in small buffers with up to  $B$  packets each (e.g.,  $B = 12$ ). DATAs  
 153 are larger packets of size  $L$  (e.g.,  $L = 9$  KB for jumbo packets),<sup>1</sup> and their buffer size equals  
 154 the remainder of the allowed buffer size. Since  $\ell \ll L$ , the queues for the small packets are  
 155 extremely unlikely to cause starvation. The packet types can be differentiated in different

<sup>1</sup> Each SIM could also generally represent a set of  $k$  DATA packets.

ways, e.g., using 2 bits out of the 6-bit ToS field in the IP header. The line rate is assumed to be  $C$  throughout the datacenter network.

**Intuition with SIMs and DATAs.** To set the token-bucket rate, we want to determine the ideal bit rates  $r_{\text{SIM}}$  for the SIMs and  $r_{\text{DATA}}$  for the DATAs. We start with a simple case where there is only one switch in the network and we can neglect the SIM and DATA acknowledgments. Assume that the flows are infinite with an infinite stream of SIMs and DATAs, such that the SIM and DATA queues are never empty after the first SIM and DATA appear. Also, let  $\alpha = \frac{L}{\ell}$ . For example, if  $L = 9$  KB and  $\ell = 64$  B, then  $\alpha \approx 141$ . We intuitively want to satisfy two conditions:

- (1) *We want to fully utilize the line capacity*, i.e.,  $r_{\text{SIM}} + r_{\text{DATA}} = C$ .
- (2) *We also want the two streams of packets to have the same packet rate*, since each successful SIM triggers a later DATA. Formally,  $\frac{r_{\text{SIM}}}{\ell} = \frac{r_{\text{DATA}}}{L}$ , yielding  $r_{\text{DATA}} = \alpha \cdot r_{\text{SIM}}$ .

Putting the two conditions together, we get

$$r_{\text{SIM}} = \frac{C}{\alpha + 1}. \quad (1)$$

Thus, by setting a token bucket of rate  $\frac{C}{\alpha+1}$  and size  $B$ , we expect to achieve these two conditions. This is confirmed in the following theorem (all proofs are in § A).

► **Theorem 1** (Ideal SIM and DATA rates). *Under the assumptions above,*

- (i) *The total rate converges to  $C$ .*
- (ii) *The SIMs and DATAs converge to a perfect alternating sequence.*

**Final scheme.** The token bucket above provides a rate of  $\frac{C}{\alpha+1}$  to SIM packets, where the  $\alpha$  factor accounts for the DATAs and the 1 accounts for the SIMs. However, it neglects the rate of SIM-ACKs and DATA-ACKs. These are harder to account for, as the rates of SIM-ACKs and DATA-ACKs depend on flows that go in the reverse direction. In addition, the DATA-ACK rate is lower as DCSIM only sends back a DATA-ACK every large number of DATAs (e.g., 16), leveraging the lack of packet losses. Since we are interested in AI collectives, we expect a mostly symmetric pattern in which the SIM-ACK rate is close to the SIM rate. Therefore, we heuristically set the token bucket rate at

$$\frac{C}{\alpha_{\text{Data}} + 1_{\text{Sim}} + 1_{\text{Sim-Ack}} + 0.1_{\text{Data-Ack}}} = \frac{C}{\alpha + 2.1}. \quad (2)$$

Evaluations show that performance is not sensitive to small variations of this heuristic factor.

## 2.4 DCSIM description

This section details the various stages of DCSIM, while using the example of Fig. 2 to illustrate each stage.

① **Sending SIM packets.** At each source host  $S$  and for each flow, let  $n_{\text{SIM}}$  denote the number of outstanding SIM and SIM-ACK packets in the network, i.e., the number of sent SIM packets for which  $S$  has neither received a SIM-ACK nor timed out. Also, let  $n_{\text{DATA}}$  denote the number of DATA packets waiting in the host to be sent. Then  $S$  always maintains the inequality

$$n_{\text{SIM}} \leq n_{\text{DATA}}, \quad (3)$$

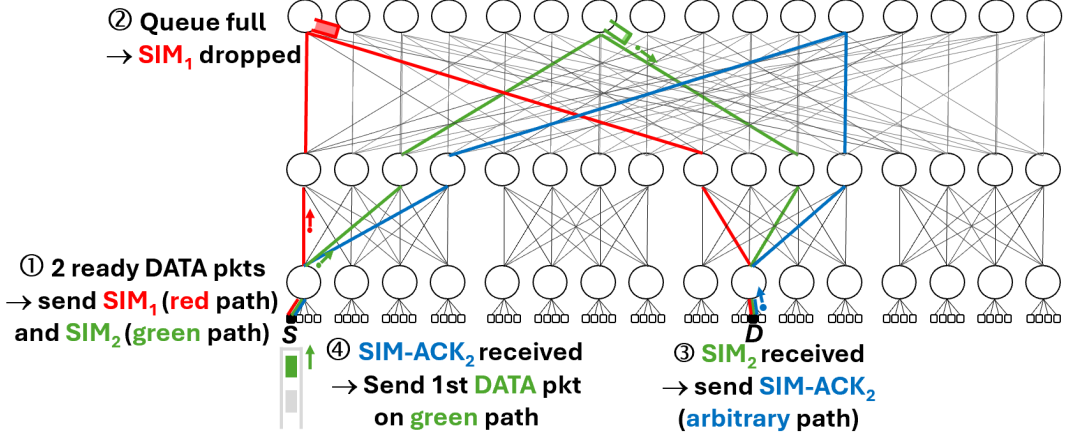


Figure 2 Example of DC-SIM operation.

i.e., it makes sure that there are no more outstanding SIMs (and SIM-ACKs) in the network than available DATAs waiting to be sent. As previously explained in § 2.3 and illustrated in Fig. 1,  $S$  maintains a SIM buffer of size  $B$  that is serviced using a token-bucket policy.  $S$  then adds SIMs to the SIM queue whenever (i) there is space in the SIM buffer, i.e., the SIM queue size is below  $B$  and (ii) there are enough DATAs to send a SIM (Equation (3)).

We have a degree of freedom in selecting the flows from which to first add SIMs. We select flows in round-robin for fairness, but could also have chosen to prioritize flows with the smallest remaining size [5]. Specifically, if there are several collectives and  $S$  knows about the collective ID of each of its flows (i.e., roughly speaking, it knows what sets of flows started together), it schedules the next SIM by checking the next collective ID in round-robin order, then choosing a SIM for the next available flow within this collective in round-robin order. If not, it simply picks flows in round-robin order.

Each new SIM is allocated a random path to the destination  $D$ . Since the datacenter network relies on commodity switches that use ECMP routing, this random-path allocation is widely implemented by allocating a unique random source port to each SIM [23, 9, 25]. DC-SIM checks that this source port is distinct from that of currently used SIMs. The source port changes the flow five-tuple of the SIM, and therefore it alters its ECMP hashed value at each switch, ultimately changing its path.

Upon transmitting a SIM on the line,  $S$  (i) records the SIM transmission time, which will also be used to send a DATA after a fixed delay; (ii) starts a timeout mechanism; and (iii) increments  $n_{\text{SIM}}$ .  $S$  also increments  $n_{\text{DATA}}$  when (i) receiving a new DATA from the operating system or (ii) a sent DATA times out without a received DATA-ACK.

**Example.** In Fig. 2, assume that at time  $t$  at source  $S$ , two DATA packets arrive at the queue for destination  $D$ , so  $n_{\text{DATA}} = 2$ .  $S$  immediately sends two SIM packets:  $\text{SIM}_1$  with a random source port that leads to the red path after ECMP hashing, then  $\text{SIM}_2$  with another random source port that leads to the green path. Thus  $n_{\text{SIM}} = n_{\text{DATA}} = 2$ .

**Switching SIM packets.** At each switch, SIM packets go through the buffer mechanism described in § 2.3. If they encounter a full SIM buffer due to simulated congestion, they are dropped. Else, they reach the destination  $D$ .

<sup>223</sup> **Example.** In Fig. 2, the SIM buffer of the leftmost core switch is full, therefore it drops  
<sup>224</sup> SIM<sub>1</sub>. In contrast, SIM<sub>2</sub> traverses the uncongested green path.

<sup>225</sup> ③ **Sending SIM-ACK packets.** When *D* receives a SIM, it immediately sends back a  
<sup>226</sup> SIM-ACK to *S*. As usual, the SIM-ACK destination port and IP address are the SIM source  
<sup>227</sup> port and IP address. Since ECMP hashing is not symmetric, the SIM-ACK can take an  
<sup>228</sup> arbitrary path after ECMP hashing of its 5-tuple, until it reaches *S*.

<sup>229</sup> **Example.** In Fig. 2, *D* receives SIM<sub>2</sub> and sends SIM-ACK<sub>2</sub> back to *S* through the blue path.

<sup>230</sup> ④ **Sending DATA packets.** When a source *S* receives a SIM-ACK for some SIM, it immediately  
<sup>231</sup> associates the SIM to the first of the DATA packets waiting in *S* to be sent. *S* updates  
<sup>232</sup>

$$\begin{cases} \text{srcPort}_{\text{DATA}} = \text{srcPort}_{\text{SIM}} \\ t_{\text{DATA}} = t_{\text{SIM}} + RTT_{\max} \end{cases} \quad (4)$$

<sup>234</sup> where the first line implies that the DATA will take the same path as its corresponding SIM,  
<sup>235</sup> and the second line means that the DATA is scheduled to be transmitted after a fixed delay  
<sup>236</sup>  $RTT_{\max}$  (defined in § 2.5) following the transmission time of its SIM. *S* also decrements  
<sup>237</sup>  $n_{\text{SIM}}$  and  $n_{\text{DATA}}$ . When sending the DATA, *S* also sets a large timer and keeps the DATA in a  
<sup>238</sup> side buffer, so that in the rare event that the DATA times out without an acknowledgment, it  
<sup>239</sup> will be inserted back at the head of the queue of DATA packets waiting to be sent.

<sup>240</sup> **Example.** In Fig. 2, *S* receives SIM-ACK<sub>2</sub>. Thus, it associates SIM<sub>2</sub> with DATA<sub>1</sub>, the first  
<sup>241</sup> DATA in the queue. If SIM<sub>2</sub> was sent at time *t*, then DATA<sub>1</sub> is later sent at time *t* +  $RTT_{\max}$   
<sup>242</sup> along the same green path. In addition, as detailed later, SIM<sub>1</sub> times out and a new SIM  
<sup>243</sup> with a new random path can be sent instead.

<sup>244</sup> Note that this example illustrates well why the association between DATA and SIM  
<sup>245</sup> packets is not made at the creation of the SIM packets, as would be intuitive. If DATA<sub>1</sub> were  
<sup>246</sup> associated to SIM<sub>1</sub>, then after SIM<sub>1</sub> is dropped, it would need to wait for a timeout and then  
<sup>247</sup> generate a new SIM, while the following DATA<sub>2</sub> packet in the queue would be released upon  
<sup>248</sup> the arrival of SIM-ACK<sub>2</sub>. This could cause severe reordering in the system.

<sup>249</sup> ⑤ **Sending DATA-ACK packets.** *D* sends a DATA-ACK back to *S* every large number of  
<sup>250</sup> DATAS (e.g., 16), leveraging the non-existent loss rate in the network (with some minimum  
<sup>251</sup> frequency, e.g., once every 3 propagation RTTs). (This is not illustrated in Fig. 2.)

<sup>252</sup> **Timeouts.** When *S* receives a DATA-ACK, it deletes the DATA. Else, as mentioned, if a  
<sup>253</sup> DATA times out, it is put back in the queue of DATAS waiting to be sent. In addition, if a  
<sup>254</sup> SIM timer expires, it decrements  $n_{\text{SIM}}$ , enabling the transmission of a new SIM.

<sup>255</sup> **Example.** In Fig. 2, when the timeout for SIM<sub>1</sub> that was set in ① expires at *t* +  $RTT_{\max}$ , *S*  
<sup>256</sup> assumes that SIM<sub>1</sub> is lost and decrements  $n_{\text{SIM}}$ . A new SIM with a new random path can  
<sup>257</sup> then be sent to *D*.

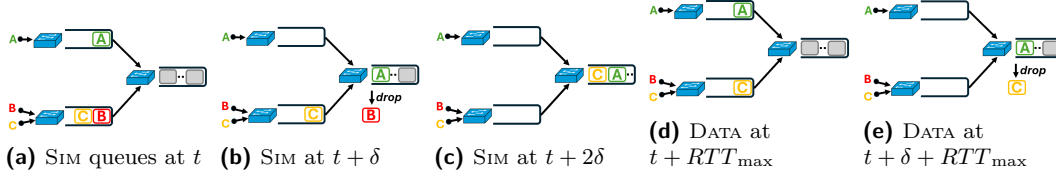


**Figure 3** Counterexample showing why DATAs may be dropped in multi-stage networks. In (a), the right-side switch SIM buffer is full. In (b), after one slot, only one SIM can access it. The SIM for  $A$  enters, so the SIM for  $B$  is dropped. In (c), after another slot, the SIM for  $C$  enters as well.  $RTT_{\max}$  later, in (d),  $A$  and  $C$  send the corresponding DATA packets. But one slot later, in (e), again only one DATA can access the limited DATA queue. No matter which one, the other DATA gets dropped even though its SIM went through.

258 **DATA management.** To summarize,  $S$  needs to manage four DATA queues, as DATAs can  
 259 be in four states: (1) at first, waiting for a SIM to be sent; then (2) after receiving a SIM-ACK,  
 260 waiting for a green light to transmit  $RTT_{\max}$  after the SIM; then (3) queued in the DATA  
 261 queue and ready to be transmitted, potentially waiting for other DATAs or SIMs currently  
 262 being transmitted; as well as (4) with a copy stored in a side buffer in case a DATA-ACK  
 263 does not come back on time and the timeout expires.

## 264 2.5 DCsim computation of $RTT_{\max}$

265 We want to compute the fixed delay  $RTT_{\max}$  between the time  $S$  transmits a SIM and the  
 266 time it transmits its corresponding DATA.  $RTT_{\max}$  is an upper bound on the SIM RTT,  
 267 i.e., the time it takes for a SIM then SIM-ACK to get from  $S$  to  $D$  then back to  $S$ . It is a  
 268 significant parameter, as it delays the transmission of DATAs to ensure synchronization, i.e.,  
 269 to make sure that DATAs experience the same lack of congestion as their corresponding SIMs.  
 270 To compute  $RTT_{\max}$ , let  $RTT_p$  denote the maximum propagation and processing time in  
 271 the datacenter network, and let  $H$  denote the maximum number of hops for SIMs from  $S$  to  
 272  $D$  or for SIM-ACKs from  $D$  to  $S$ . Then we obtain:

273 ▶ **Theorem 2.** *The SIM round-trip time is no more than*

$$274 \quad RTT_{\max} = RTT_p + \frac{2H \cdot \ell}{C} \cdot ((B + 1) \cdot \alpha + 2.1B + 1) \quad (5)$$

275 Typically, we would expect this upper bound  $RTT_{\max}$  to be within  $1 - 1.5 \times$  the propagation  
 276 RTT for 1.5 KB DATA packets, but it can be larger for larger packets.

277 **Example.** Assume that  $H = 6$  hops in a three-level fat-tree topology,  $RTT_p = 7.8 \mu\text{s}$ ,  
 278  $C = 800 \text{ Gbps}$ ,  $L = 1.5 \text{ KB}$ ,  $\ell = 64 \text{ B}$ , and  $B = 12 \text{ pkts}$ . Then  $\alpha = \frac{1,500}{64} = 23$  and  
 279  $RTT_{\max} = 1.32 RTT_p = 10.3 \mu\text{s}$ .

## 280 3 DCsim Properties

281 In this section, we present fundamental results about DCsim properties. First, we show that  
 282 in DCsim, counter-intuitively, SIMs may traverse a buffer even though their corresponding  
 283 DATAs will not. This goes against the fact that there are no more DATAs than SIMs, and  
 284 therefore the expectation that DATAs will experience less congestion. Second, we prove that  
 285 the token bucket of size  $B$  tokens for SIMs can be reduced to a size of two tokens only without  
 286 hurting the property that SIMs and DATAs can alternate at full rate.

### 287 3.1 The limits of emulation

288 We now want to demonstrate that while in a single switch buffer, SIMs and DATAs can  
 289 converge to an ideal schedule where SIMs and DATAs alternate without drops and the link  
 290 becomes fully utilized (Theorem 1), this does not hold in general in a datacenter network.

291 **Counterexample.** Let's provide intuition for why we cannot generalize results from a single  
 292 switch to the whole network. As explained in § 2.2, a SIM denoted  $SIM_0$  may compete with  
 293 other SIMs for a place in the SIM queue. However, these other SIMs may be dropped in later  
 294 switches, completely changing the timing and effectively canceling the effects of reservation.  
 295 Thus, when the  $DATA_0$  corresponding to  $SIM_0$  arrives after  $RTT_{max}$ , it may not need to  
 296 compete with other DATAs anymore, because their SIMs were dropped. Hence, it may quickly  
 297 exit the switch and arrive earlier than  $SIM_0$  at the next switch. However, the next switch  
 298 may currently be congested, leading to  $DATA_0$  being dropped.

299 Fig. 3 illustrates a counterexample, assuming the DATA buffer can only hold  $B$  packets  
 300 like the SIM buffer. It follows a switch buffer slot-by-slot, where each slot of duration  $\delta$   
 301 corresponds to the time between tokens in the SIM token-buffer mechanism (i.e.,  $\delta = \frac{L+2,1\ell}{C}$ ,  
 302 following Equation (2)). It shows that while the SIM for source host  $C$  goes through the  
 303 switch seamlessly, its DATA actually needs to be dropped.

304 **DATA buffer size.** In practice, the above counterexample means that we can only expect  
 305 a practical near-zero loss rate, not a deterministic zero-loss guarantee. For example, in  
 306 evaluations (§ 4), we found that if the DATA buffer can hold about  $2\times$  as many packets as  
 307 the SIM buffer, then *we could not see a single DATA loss*, no matter the traffic pattern and  
 308 the network oversubscription.

### 309 3.2 Token bucket size

310 Since SIMs have higher priority in the switches, they have precedence over all other traffic  
 311 classes. However, because of the non-preemption, they will be delayed if a DATA is currently  
 312 being sent. Still, they can at most be delayed by the time  $\frac{L}{C}$  to send a DATA. The following  
 313 theorem shows that if we want to reach an alternating sequence of SIMs and DATAs at line  
 314 rate as proved in Theorem 1 (and under the same assumptions), we cannot use a token-bucket  
 315 size of 1, as it would reduce the SIM rate, while any size above 2 is fine.

316 ▶ **Theorem 3 (Token bucket).** *To achieve an alternating sequence of SIMs and DATAs at line  
 317 rate, it is necessary and sufficient to have a token-bucket size of at least 2.*

## 318 4 DCSIM Evaluation

319 We evaluate DCSIM through extensive simulations, which reveal the following key results vs.  
 320 other algorithms:

- 321 ■ **Zero loss.** Throughout the evaluations with a regular DATA buffer size, DCSIM experiences  
 322 zero loss.
- 323 ■ **Higher Utilization.** DCSIM achieves a 12% increase in utilization with an all-to-all  
 324 traffic pattern. Moreover, DCSIM maintains a negligible reordering size.
- 325 ■ **Lower CCT.** DCSIM achieves up to 10% lower CCT under a mix of five all-to-all-v  
 326 collectives. It still outperforms other algorithms while varying the packet sizes, buffer  
 327 sizes, flow sizes, collective sizes, and number of collectives.

328 ■ **Oversubscribed network.** DCsim shines under adverse conditions. In an oversubscribed  
 329 scenario with only half the core switches, its CCT is 45% that of other algorithms, and it  
 330 experiences no losses while their loss rates are typically above 10%.

331 **4.1 Setup**

332 **Algorithms.** We implement DCsim in the dcPIM simulator [55], and evaluate it against  
 333 dcPIM, pHost and pFabric.<sup>2</sup> The DCsim source code is available online [53].

334 **Topology.** We employ a 3-layer fat-tree topology [4] with a switch radix  $k = 8$ , resulting  
 335 in a network consisting of 128 end-hosts, 32 edge switches, 32 aggregation switches, and 16  
 336 core switches. All links are configured with 800 Gbps bandwidth, as commercially available  
 337 today [40], and jumbo frames of 9 KB. We use the simulator default settings for the other  
 338 parameters: each link propagation delay is set to 200 ns, and each switch is configured with  
 339 a buffer size of 500 KB per port and a processing latency of 450 ns, yielding a zero-load  
 340 RTT of  $7.8\mu\text{s}$ . For DCsim, we set a constant SIM buffer size of  $B = 12$  packets, reflecting our  
 341 goal of keeping low queueing occupancies. When evaluating small buffer sizes below 250 KB  
 342 (equivalent to 28 DATA packets), we reduce  $B$  proportionally to the buffer size, ensuring that  
 343 the SIM and DATA buffer sizes decrease in lockstep.

344 **Oversubscribed topology.** We also test the algorithms using an oversubscribed (blocking)  
 345 topology [54] where half the core switches are removed.

346 **Collectives.** We focus on collective communication patterns that are representative of AI  
 347 training workloads, and add the functionality to the simulator. A *collective* is defined as a  
 348 set of flows that begin transmission simultaneously. We implement the following collectives:

349 **(1) Permutation.** The permutation pattern models a *ring all-reduce* collective algorithm.  
 350 Each sender sends a single flow to a single receiver, and each receiver receives a single flow  
 351 from a single sender, yielding a total of  $n$  flows when there are  $n$  hosts in the collective. Each  
 352 single collective always uses all the hosts ( $n = 128$ ).

353 **(2) All-to-all.** The all-to-all pattern models *tensor parallelism*. All hosts in the collective  
 354 send a flow to all other hosts, yielding  $n(n - 1)$  flows per collective of size  $n$ . We also evaluate  
 355 an *infinite* all-to-all workload where each flow has an infinite size.

356 **(3) All-to-all-v.** The all-to-all variable (all-to-all-v) pattern models *mixture of experts (MoE)*  
 357 traffic [33, 32, 21, 22, 13, 30, 51]. It is similar to all-to-all, but can be highly unbalanced.  
 358 To model it, each packet from each sender chooses a random receiver out of the  $n - 1$  other  
 359 hosts in the collective.

360 **(4) Set of all-to-all-v.** To reflect several competing MoE collectives or tenants, we also  
 361 focus on a set of several collectives of different sizes that operate in the same datacenter  
 362 network, as competing collectives are known to be hard to service [49, 32, 26, 58]. We define  
 363 a baseline set as using all-to-all-v with 5 collectives, with collective sizes randomly selected

---

<sup>2</sup> dcPIM has been shown [10] to have superior performance vs. Homa [37], Aeolus [19], NDP [17, 48] and HPCC [29] in various settings, therefore we do not repeat comparisons against these algorithms.

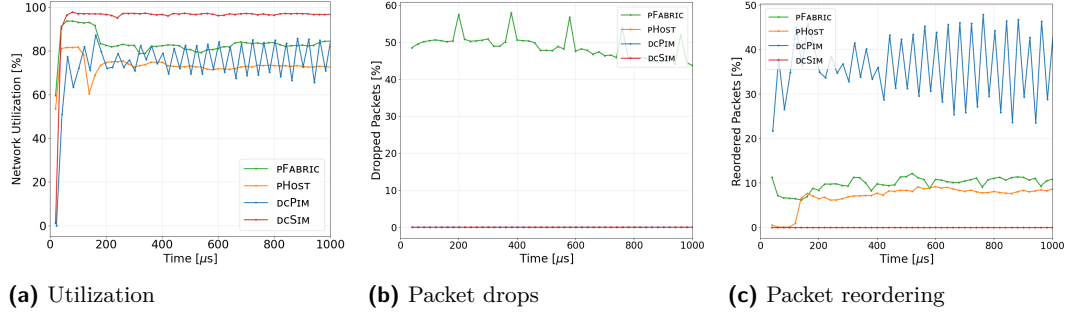


Figure 4 Single all-to-all collective with infinite flows.

364 from the set  $\{8, 16, 32, 64\}$ , possibly with hosts sharing several collectives, and flow sizes of  
 365  $2 \times$  bandwidth-delay product (BDP). We then vary these parameters to study their impact.

366 **Metrics.** We measure the: (1) *Collective completion time (CCT)*, i.e., the time at which  
 367 the last packet of a collective reaches its destination. When there are several collectives, we  
 368 average over all CCTs. (2) *Packet loss rate*. (3) *Total queueing delay*, i.e., the total time  
 369 from the transmission time at the source host to arrival time at the destination host for data  
 370 packets. (4) *Reordering size*, i.e., the number of data packets per measurement interval that  
 371 arrive at the destination with non-maximal sequence number. We measure it because in the  
 372 selective-repeat algorithm and in practical hardware implementations, when there is high  
 373 reordering, the difference between the sent and received orders of several packets can exceed  
 374 the transmit window, thus throttling throughput and leading to network underutilization.  
 375 (5) *Utilization*, i.e., the quantity of data received in a time interval, divided by the total link  
 376 capacity of the hosts.

377 We run each simulation 20 times and plot the average result, together with the standard  
 378 error of the mean (SEM) as error bars.

## 379 4.2 Performance evaluation

380 **Infinite all-to-all.** Fig. 4 illustrates the performance of DCsim compared to dcPIM, pFabric  
 381 and pHOST in an infinite all-to-all traffic pattern. The network utilization of DCsim remains  
 382 higher than in the other algorithms by at least 14% (Fig. 4(a)). The lower utilization of  
 383 pFabric may be due to its high level of packet drops. DCsim also impressively achieves 0%  
 384 loss and 0% packet reordering at all times (Figs. 4(b) and 4(c)). DCsim's low reordering  
 385 throughout the evaluations may be due to two main reasons. First, its lower queueing delay,  
 386 as seen in several evaluations. Second, the fact that when sending a burst of SIMs through  
 387 several paths then receiving the SIM-ACKs back, DATAs are later selected in the order in  
 388 which SIM-ACKs were received, e.g., the first DATA is sent on the shortest path. It makes it  
 389 less likely for a later DATA to pull ahead. In contrast, dcPIM and pHOST are able to remain  
 390 lossless, but decrease their sending rate as they detect congestion in the network, based on  
 391 received token packets.

392 **Single permutation and single all-to-all.** Fig. 5 illustrates the CCT with either a single  
 393 permutation or a single all-to-all collective for different flow sizes. The flow sizes are presented  
 394 as multiples of BDP, where BDP represents 87 packets. As expected, for all algorithms,  
 395 CCT increases when the flow size increases. DCsim completes faster than dcPIM, pFabric

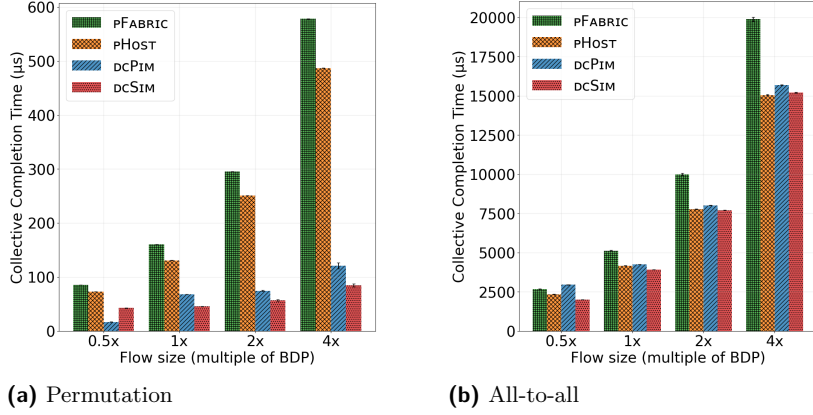


Figure 5 Single permutation or all-to-all collective with different flow sizes.

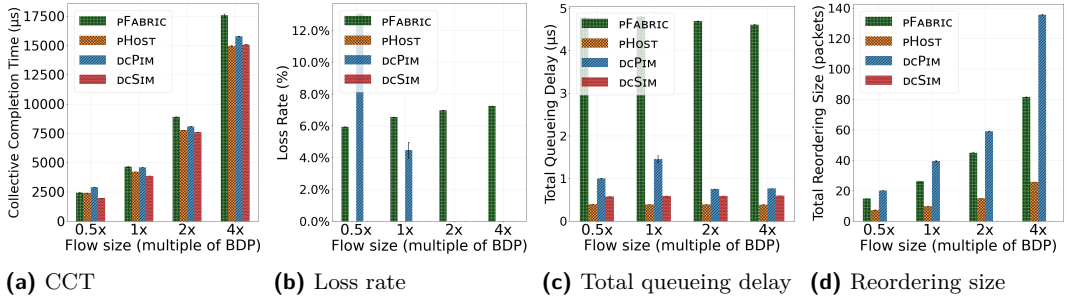


Figure 6 Single all-to-all-v collective with different average flow sizes.

and pHost in all experiments, except for an half-BDP size in the permutation traffic. This evaluation is the least congested of all. Under 1 BDP, dcPIM does not activate its full algorithm for small flows, and therefore simply sends the flows without any control packets. DCSIM's focus is on larger flows for AI training, but it could adopt the same behavior for small flows by sending them at a lower priority without using SIM packets. Above 1 BDP, the dcPIM algorithm is activated, worsening the CCT. On the other hand, with the heavier all-to-all traffic (Fig. 5(b)), the non-activation of dcPIM for short flows of size  $0.5 \times$  BDP increases dcPIM's CCT even beyond that of pFabric and pHost.

**Single all-to-all-v.** Fig. 6 presents the results of running a single all-to-all-v collective as a function of different average flow sizes. Since flow sizes vary, we only consider their average, and express it again as a multiple of BDP. DCSIM uniformly achieves lower CCTs, with an average improvement of 12.5%, together with a zero loss rate and reordering size, and a small queueing delay.

**Several all-to-all-v.** Fig. 7 presents an evaluation with five concurrent collectives of random sizes. Performance is largely similar to a single all-to-all-v, with a non-zero yet negligible reordering size. Given the lower total load, dcPIM's queueing delay also gets lower and similar to DCSIM. pHost achieves the lowest queueing delay due to its conservative schedule, which comes at the cost of a higher CCT.

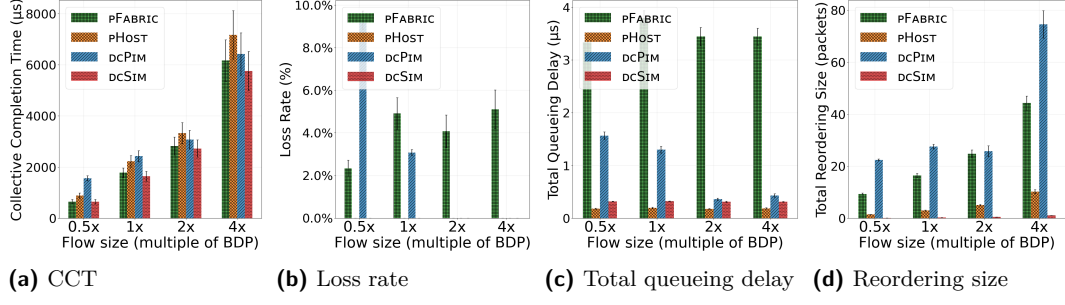


Figure 7 Five all-to-all-v collectives with different average flow sizes.

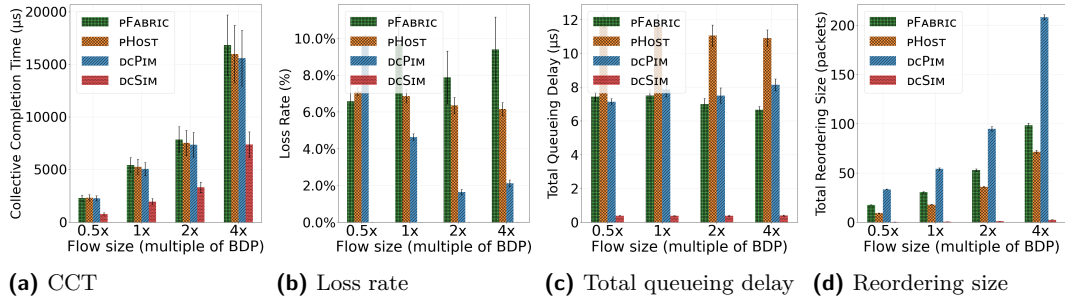


Figure 8 Adverse scenario with an oversubscribed network using half the core switches, given five all-to-all-v collectives.

414 **Oversubscribed all-to-all-v.** Fig. 8 illustrates an adverse scenario with an oversubscribed  
 415 network in the baseline scenario of five all-to-all-v collectives. We effectively halve the number  
 416 of core switches by retaining only the odd-indexed switches and reducing the rate of the  
 417 remaining one to 1% of their initial rate. DCSIM excels in this case, with markedly better  
 418 performance than the other algorithms. The simulation phase enables DCSIM to detect and  
 419 avoid congested paths by dropping SIM packets early, thereby preventing subsequent DATA  
 420 packet losses. In contrast, dcPIM schedules end-to-end links between two hosts but cannot  
 421 identify whether one path is better than another, since it has no visibility inside the network.  
 422 Some aggregation switches are much more congested than others, therefore load-balancing  
 423 cannot be made blindly. Once congestion is detected, dcPIM reduces the total sending rate  
 424 to limit losses, but then does not utilize the full network capacity.

### 425 4.3 Sensitivity analysis

426 We now perform a sensitivity analysis for the topology parameters by varying a single  
 427 parameter each time.

428 **Packet size.** Fig. 9(a) compares the CCT when using some of the most common DATA  
 429 packet sizes in datacenter networks: 1.5 KB (Ethernet), 4 KB (RDMA), or 9 KB (Jumbo).  
 430 As expected, for all algorithms, the CCT is lower when  $L$  is higher, i.e., larger packets help  
 431 with bulky transfers. While we used 9 KB as the default packet size in our evaluations,  
 432 DCSIM actually outperforms other algorithms even more for lower packet sizes.

433 **Underbuffering.** Fig. 9(b) illustrates the impact of reducing the switch buffer sizes. DCSIM  
 434 is resilient to this reduction, and results are largely similar to previous evaluations.

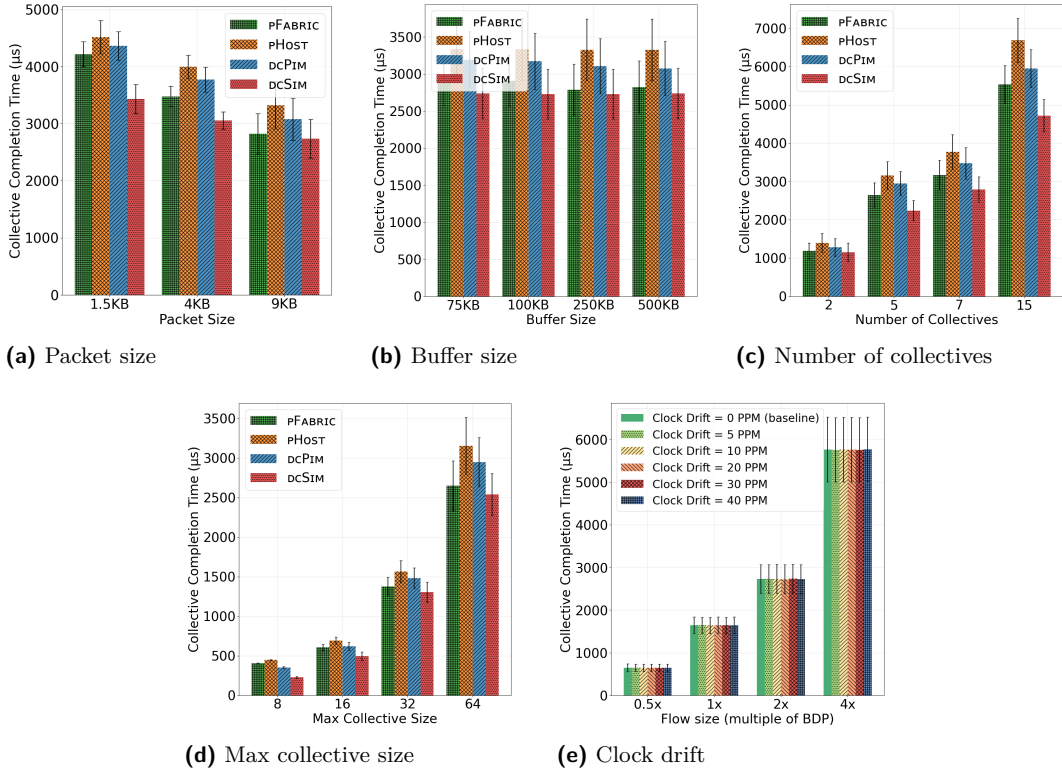


Figure 9 Sensitivity analysis to topology parameters

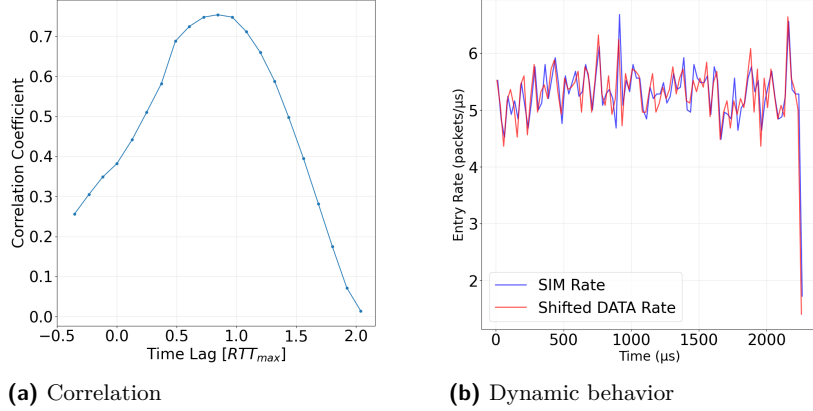
435 **Number of collectives.** Fig. 9(c) varies the number of all-to-all-v collectives. DCSIM keeps  
 436 outperforming, and outperforms even more at high loads with many collectives.

437 **Max collective size.** Fig. 9(d) illustrates the impact of the maximum collective size, given  
 438 five random all-to-all-v collectives. DCSIM keeps outperforming in all cases.

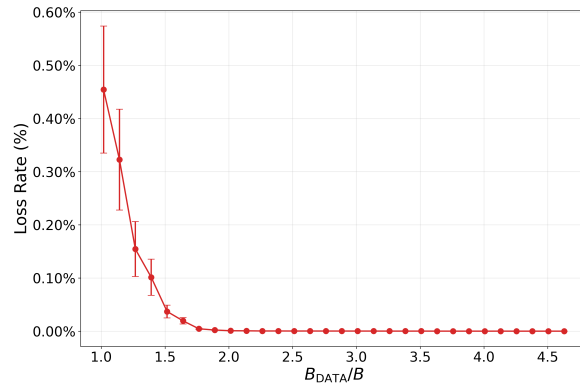
439 **Clock drift.** We rely on an  $RTT_{max}$  delay given by an internal clock. We evaluated the  
 440 resilience of our system to clock drift using a methodology similar to that employed in  
 441 Firefly [28]. Fig. 9(e) demonstrates that the impact on CCT remains negligible, with a  
 442 performance degradation of less than 1% even under a static drift of 40 PPM.

#### 443 4.4 DCSIM properties

444 **Correlation of SIM and DATA.** Fig. 10(a) illustrates the correlation in a random last-hop  
 445 switch between the rate of SIM packets and the rate of DATA packets with shifted times, in  
 446 order to verify that the rate of DATA packets corresponds indeed to the earlier rate of SIM  
 447 packets. We consider a last-hop (edge switch → host) switch queue to reduce the impact  
 448 of SIMs that may be later dropped. The correlation achieves a maximum value of 0.77,  
 449 confirming that the DATA rate indeed reflects the SIM rate, even though the match is not  
 450 entirely perfect. In addition, the corresponding time lag is 0.86  $RTT_{max}$ . The intuition for a  
 451 lag lower than  $RTT_{max}$  is that the SIM drops along the path lead to lower queueing delay  
 452 for the DATAs, which reach the last-hop queue faster.



■ **Figure 10** SIMS vs. lagged DATAs at the last hop. (a) Correlation between the SIM and time-shifted DATA rates. (b) Dynamic behavior of SIM queue and time-shifted DATA queue.



■ **Figure 11** DCsim loss rate as a function of  $\frac{B_{Data}}{B}$ .

453 In addition, Fig. 10(b) shows the dynamic behavior of the SIM and (lagged) DATA queues.  
 454 They clearly tend to move together consistently, indicating that it is not unreasonable to  
 455 assume in general that if the SIM buffer is not congested, then neither should the DATA  
 456 buffer.

457 **DATA buffer.** Fig. 11 shows the impact of the DATA buffer size on the loss rate, given a  
 458 constant SIM buffer size that can hold  $B = 12$  SIM packets. Let  $B_{Data}$  denote the number of  
 459 DATAs that can fit in the DATA buffer size. Then the figure shows that for

$$460 \quad \frac{B_{Data}}{B} \geq 2, \quad (6)$$

461 there is no loss, i.e., if the DATA buffer can fit 24 DATAs, no DATA will be lost despite the high  
 462 load of five all-to-all-v collectives. While the lossless threshold is not at an ideal  $\frac{B_{Data}}{B} = 1$   
 463 that would correspond to an exact emulation, it is still an impressive result that the network  
 464 can run lossless with so little buffering.

465 **Async DCsim.** DCsim sends each DATA packet  $RTT_{max}$  after its corresponding SIM was  
 466 sent. We introduce an *Async DCsim* version that acts impatiently and immediately sends the  
 467 DATA packet after a SIM-ACK arrives at the source. Async DCsim is intriguing, because on

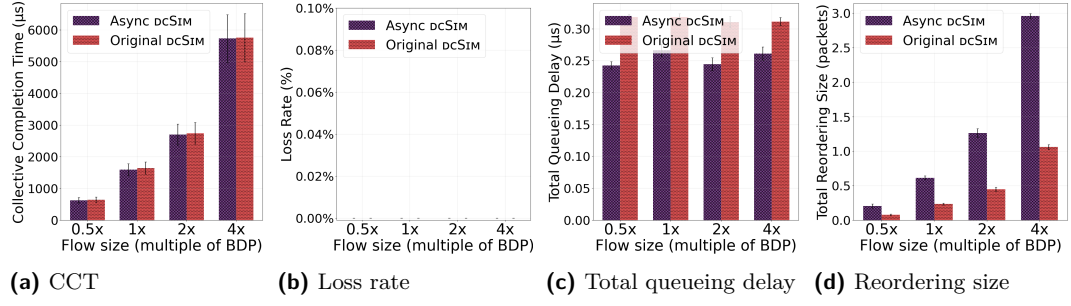


Figure 12 Async dcSIM vs. original dcSIM.

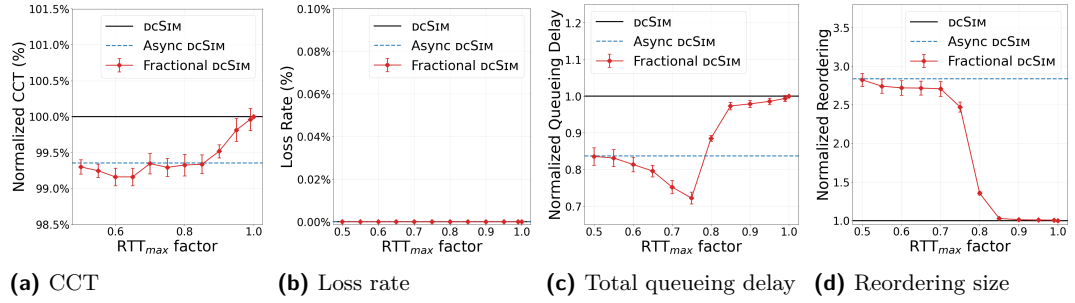


Figure 13 Fractional dcSIM vs. baseline dcSIM and Async dcSIM

468 the one hand, it loses the theoretical synchronization, but on the other, it is more reactive to  
 469 changes in network conditions.

470 Fig. 12 shows how the CCT of Async dcSIM is slightly lower than the CCT of the regular  
 471 dcSIM. Its loss rate is also 0%, and its queueing delay is lower by up to 24%, as it is more  
 472 likely to quickly exploit a low queue size. However, since it is not synchronized anymore,  
 473 its number of reordered packets becomes much higher, indicating a higher disparity in the  
 474 queue sizes between different paths. Thus, this Async version offers different tradeoffs for  
 475 the datacenter operator.

476 **Fractional dcSIM.** dcSIM waits  $RTT_{max}$  to send DATA packets, where  $RTT_{max}$  is com-  
 477 puted according to the worst-case formula of Theorem 2. Motivated by the findings in Async  
 478 dcSIM, we analyze the impact on system performance of only waiting for a fraction of the  
 479 worst-case  $RTT_{max}$ . More specifically, we send the DATA packet at the later of (1) this  
 480 fractional delay following the SIM transmission and (2) the SIM-ACK arrival time.

481 Fig. 13 compares this fractional dcSIM for several fractional  $RTT_{max}$  values against  
 482 the original dcSIM and Async dcSIM. It shows that the CCT of the fractional dcSIM is  
 483 marginally lower than for the baseline dcSIM, while its packet loss remains at 0%. In addition,  
 484 its queueing delay decreases. However, packet reordering increases, maybe because we are  
 485 slowly losing the guarantee provided by  $RTT_{max}$ . We observe that queueing and reordering  
 486 behavior remain comparable to the baseline dcSIM from  $RTT_{max}$  down to 0.85  $RTT_{max}$ ,  
 487 while the behavior converges towards that of Async dcSIM as  $RTT_{max}$  is further reduced.

## 488 5 Related Work

489 Table 1 provides a qualitative comparison of dcSIM against existing transport paradigms, as  
 490 detailed below.

Type	Handles network congestion	Practically lossless	Handles low-rate flows	Uses commodity switches
Load balancing (Oblivious spraying, REPS)	✓	✗	✓	✓
Credits (ExpressPass)	✗	✗	✓	✓
Scheduling (dcPIM, pHost)	✗	✗	✓	✓
Reservation (Harmony)	✓	✓	✗	✗
Simulation probe (dcSIM)	✓	✓	✓	✓

Table 1 Comparison of datacenter transport designs.

491 **Per-packet load-balancing.** Many solutions use per-packet load balancing with commodity  
 492 switches [12, 59, 18, 34, 25, 9, 8, 56, 47, 1, 39, 57, 41, 50]. They rely on diverse reliability  
 493 mechanisms [16, 38, 52, 8, 42, 56]. However, the RoCE-like recovery schemes can experience  
 494 poor performance with high per-flow rates, and trimming-based schemes can degrade with  
 495 many flows [36]. Such load-balancing schemes can also suffer from the interaction with  
 496 congestion control [15].

497 **Receiver-driven credits.** ExpressPass [11] introduces a receiver-driven credit-based scheme  
 498 that attempts to avoid losses, but it relies on switch modifications, e.g., to ensure symmetric  
 499 paths, and cannot handle multi-path and link failures. Additional credit-based algorithms,  
 500 like Homa [37], Aeolus [19] and FlexPass [31], often have little visibility into the network.

501 **Scheduling.** pHost [14] shifts scheduling decisions to end hosts using Request-to-Send (RTS)  
 502 and token-based coordination, avoiding switch modifications. It can be seen as implementing  
 503 a single stage of matching. While simpler to deploy, its coordination mechanism can incur  
 504 overhead under bursty or high fan-in patterns. dcPIM [10] replaces  $\log(n)$  matching rounds  
 505 from classical PIM with constant-time matching, achieving high utilization and scalability.  
 506 However, it does not have visibility within the network.

507 **Priorities.** pFabric [5] is a seminal design that prioritizes packets from flows with the  
 508 smallest remaining size. In contrast, DCSIM adopts a round-robin policy.

509 **Non-commodity hardware.** Additional schemes show potential for avoiding losses, but re-  
 510 quire non-commodity hardware. HPCC [29] uses in-network telemetry to provide fine-grained,  
 511 real-time congestion feedback for precise end-host rate control, but relies on programmable  
 512 switch support and accurate timestamping, which may not be universally available. Rate-  
 513 less erasure coding can mask losses but needs specialized NICs to be implemented at high  
 514 rates [24, 36]. Harmony [3] relies on per-flow fixed-bandwidth reservations to eliminate  
 515 congestion-related drops while achieving high utilization, but needs specialized switches to  
 516 participate in the reservation process, and struggles with low-rate and variable-rate flows  
 517 that do not match the fixed reservation rates.

518 **Lossless networks.** Large lossless networks have been deployed in datacenter networks [6]  
 519 and constitute an alternative to lossy networks.

520 **6 Conclusion**

521 In the paper we introduced DCSIM, a novel transport algorithm that achieves low CCTs  
522 and *practically lossless* performance with commodity switches. DCSIM relies on a paradigm  
523 shift, by simulating the result of going through a path before doing it. In DCSIM, each  
524 packet first employs a small simulation probe to traverse the network and explore congestion  
525 along a candidate path. Only packets whose simulation probes succeed are then transmitted,  
526 expecting to succeed as well. Evaluations confirmed that DCSIM achieves faster CCTs and  
527 higher utilization than existing schemes, with small queues and virtually zero packet loss.  
528 Finally, evaluations showed how DCSIM remains effective under adverse conditions that are  
529 highly challenging and cause many losses in other algorithms.

530 **References**

- 531 1 D. Abts and J. Kim. *High Performance Datacenter Networks: Architectures, Algorithms,*  
532 *and Opportunities*. Synthesis Lectures on Computer Architecture. Springer International  
533 Publishing, 2022. URL: <https://books.google.ca/books?id=NYZyEAAQBAJ>.
- 534 2 Sharon Adar. Amazon Is Building a Gigantic Computing Facility to Match the Human  
535 Brain. <https://futurism.com/the-byte/amazon-anthropic-ai-data-center>, 2025.
- 536 3 Saksham Agarwal, Qizhe Cai, Rachit Agarwal, David Shmoys, and Amin Vahdat. Harmony:  
537 A congestion-free datacenter architecture. In *Usenix NSDI*, pages 329–343, 2024.
- 538 4 Mohammad Al-Fares, Alexander Loukissas, and Amin Vahdat. A scalable, commodity data  
539 center network architecture. In *ACM SIGCOMM*, pages 63–74, 2008. doi:10.1145/1402958.  
540 1402967.
- 541 5 Mohammad Alizadeh, Shuang Yang, Milad Sharif, Sachin Katti, Nick McKeown, Balaji  
542 Prabhakar, and Scott Shenker. pFabric: Minimal Near-Optimal Datacenter Transport. In  
543 *SIGCOMM*, 2013.
- 544 6 Wei Bai, Shanim Sainul Abdeen, Ankit Agrawal, Krishan Kumar Attre, Paramvir Bahl, Ameya  
545 Bhagat, Gowri Bhaskara, Tanya Brokhman, Lei Cao, Ahmad Cheema, et al. Empowering  
546 Azure Storage with RDMA. In *Usenix NSDI*, 2023.
- 547 7 Matthias Bastian. OpenAI’s Stargate pivot highlights rift with Microsoft over future AI  
548 computing needs. <https://the-decoder.com/openais-stargate-pivot-highlights-rift-with-microsoft-over-future-ai-computing-needs/>, 2025.
- 549 8 Tommaso Bonato, Abdul Kabbani, Daniele De Sensi, Rong Pan, Yanfang Le, Costin Ra-  
550 riciu, Mark Handley, Timo Schneider, Nils Blach, Ahmad Ghalayini, et al. FASTFLOW:  
551 Flexible Adaptive Congestion Control for High-Performance Datacenters. *arXiv preprint*  
552 *arXiv:2404.01630*, 2024.
- 553 9 Tommaso Bonato, Abdul Kabbani, Ahmad Ghalayini, Michael Papamichael, Mohammad  
554 Dohadwala, Lukas Gianinazzi, Mikhail Khalilov, Elias Achermann, Daniele De Sensi, and  
555 Torsten Hoefer. REPS: Recycled entropy packet spraying for adaptive load balancing and  
556 failure mitigation. In *EuroSys*, 2026.
- 557 10 Qizhe Cai, Mina Tahmasbi Arashloo, and Rachit Agarwal. dcPIM: Near-optimal proactive  
558 datacenter transport. In *ACM SIGCOMM*, pages 53–65, 2022.
- 559 11 Inho Cho, Keon Jang, and Dongsu Han. Credit-scheduled delay-bounded congestion control  
560 for datacenters. In *ACM SIGCOMM*, pages 239–252, 2017.
- 561 12 Advait Dixit, Pawan Prakash, Y Charlie Hu, and Ramana Rao Kompella. On the impact of  
562 packet spraying in data center networks. In *IEEE Infocom*, pages 2130–2138, 2013.
- 563 13 Adithya Gangidi, Rui Miao, Shengbao Zheng, Sai Jayesh Bondu, Guilherme Goes, Hany Morsy,  
564 Rohit Puri, Mohammad Riftadi, Ashmitha Jeevaraj Shetty, Jingyi Yang, et al. RDMA over  
565 Ethernet for distributed training at Meta scale. In *ACM SIGCOMM*, pages 57–70, 2024.
- 566 14 Peter X. Gao, Akshay Narayan, Gautam Kumar, Rachit Agarwal, Sylvia Ratnasamy, and  
567 Scott Shenker. pHost: Distributed near-optimal datacenter transport over commodity network

569 fabric. In *ACM CoNEXT*, pages 1–12. ACM, 2015. URL: <https://dl.acm.org/doi/10.1145/2716281.2836086>, doi:10.1145/2716281.2836086.

570

571 15 Barak Gerstein, Mark Silberstein, and Isaac Keslassy. Making congestion control robust to  
572 per-packet load balancing in datacenters, 2025. arXiv:2509.07907. URL: <https://arxiv.org/abs/2509.07907>.

573

574 16 Chuanxiong Guo, Haitao Wu, Zhong Deng, Gaurav Soni, Jianxi Ye, Jitu Padhye, and Marina  
575 Lipshteyn. RDMA over commodity ethernet at scale. In *ACM SIGCOMM*, pages 202–215,  
576 2016.

577 17 Mark Handley, Costin Raiciu, Alexandru Agache, Andrei Voinescu, Andrew W Moore, Gianni  
578 Antichi, and Marcin Wójcik. Re-architecting datacenter networks and stacks for low latency  
579 and high performance. In *ACM SIGCOMM*, pages 29–42, 2017.

580 18 Jinbin Hu, Jiawei Huang, Wenjun Lv, Yutao Zhou, Jianxin Wang, and Tian He. CAPS: Coding-  
581 based adaptive packet spraying to reduce flow completion time in data center. *IEEE/ACM  
582 Transactions on Networking*, 27(6):2338–2353, 2019.

583 19 Shuihai Hu, Wei Bai, Gaoxiong Zeng, Zilong Wang, Baochen Qiao, Kai Chen, Kun Tan, and  
584 Yi Wang. Aeolus: A building block for proactive transport in datacenters. In *ACM SIGCOMM*,  
585 pages 422–434, 2020.

586 20 Gadi Hutt and Bob Evans. AWS Launches Project Rainier: Massive AI Supercomputing  
587 Cluster for Anthropic. <https://podcasts.apple.com/bb/podcast/aws-launches-project-rainier-massive-ai-supercomputing/id1437752008?i=1000717513092>, 2025.

588

589 21 Albert Q Jiang, Alexandre Sablayrolles, Antoine Roux, Arthur Mensch, Blanche Savary, Chris  
590 Bamford, Devendra Singh Chaplot, Diego de las Casas, Emma Bou Hanna, Florian Bressand,  
591 et al. Mixtral of experts. *arXiv preprint arXiv:2401.04088*, 2024.

592 22 Zewen Jin, Shengnan Wang, Jiaan Zhu, Hongrui Zhan, Youhui Bai, Lin Zhang, Zhenyu Ming,  
593 and Cheng Li. Bigmac: A communication-efficient mixture-of-experts model structure for fast  
594 training and inference, 2025. URL: <https://arxiv.org/abs/2502.16927>, arXiv:2502.16927.

595 23 Naga Katta, Aditi Ghag, Mukesh Hira, Isaac Keslassy, Aran Bergman, Changhoon Kim,  
596 and Jennifer Rexford. Clove: Congestion-aware load balancing at the virtual edge. In *ACM  
597 CoNEXT*, pages 323–335, 2017.

598 24 Mikhail Khalilov, Siyuan Shen, Marcin Chrapek, Tiancheng Chen, Kenji Nakano, Peter-  
599 Jan Gootzen, Salvatore Di Girolamo, Rami Nudelman, Gil Bloch, Sreevatsa Anantharamu,  
600 et al. SDR-RDMA: Software-defined reliability architecture for planetary scale RDMA  
601 communication. *arXiv preprint arXiv:2505.05366*, 2025.

602 25 Yanfang Le, Rong Pan, Peter Newman, Jeremias Blendin, Abdul Kabbani, Vipin Jain, Raghava  
603 Sivaramu, and Francis Matus. Strack: A reliable multipath transport for AI/ML clusters.  
604 *arXiv preprint arXiv:2407.15266*, 2024.

605 26 Jiamin Li, Yimin Jiang, Yibo Zhu, Cong Wang, and Hong Xu. Accelerating distributed MoE  
606 training and inference with lina. In *2023 USENIX Annual Technical Conference (USENIX  
607 ATC 23)*, pages 945–959, 2023.

608 27 Wenxue Li, Xiangzhou Liu, Yunxuan Zhang, Zihao Wang, Wei Gu, Tao Qian, Gaoxiong Zeng,  
609 Shoushou Ren, Xinyang Huang, Zhenghang Ren, et al. Revisiting RDMA reliability for lossy  
610 fabrics. In *ACM SIGCOMM*, pages 85–98, 2025.

611 28 Yuliang Li et al. Firefly: Scalable, ultra-accurate clock synchronization for datacenters. In  
612 *ACM SIGCOMM*, pages 434–452, 2025.

613 29 Yuliang Li, Rui Miao, Hongqiang Harry Liu, Yan Zhuang, Fei Feng, Lingbo Tang, Zheng  
614 Cao, Ming Zhang, Frank Kelly, Mohammad Alizadeh, and Minlan Yu. HPCC: High precision  
615 congestion control. In *ACM SIGCOMM*, pages 44–58, 2019.

616 30 Xudong Liao, Yijun Sun, Han Tian, Xinchen Wan, Yilun Jin, Zilong Wang, Zhenghang  
617 Ren, Xinyang Huang, Wenxue Li, Kin Fai Tse, et al. MixNet: A runtime reconfigurable  
618 optical-electrical fabric for distributed mixture-of-experts training. In *ACM SIGCOMM*, pages  
619 554–574, 2025.

620 31 Hwijoon Lim, Jaehong Kim, Inho Cho, Keon Jang, Wei Bai, and Dongsu Han. Flexpass: A  
 621 case for flexible credit-based transport for datacenter networks. In *EuroSys*, pages 606–622,  
 622 2023.

623 32 Wei Liu, Kun Qian, Zhenhua Li, Tianyin Xu, Yunhao Liu, Weicheng Wang, Yun Zhang,  
 624 Jiakang Li, Shuhong Zhu, Xue Li, et al. SkeletonHunter: Diagnosing and localizing network  
 625 failures in containerized large model training. In *ACM SIGCOMM*, pages 527–540, 2025.

626 33 Xinyi Liu, Yujie Wang, Fangcheng Fu, Xupeng Miao, Shengan Zhu, Xiaonan Nie, and Bin Cui.  
 627 NetMoE: Accelerating MoE training through dynamic sample placement. In *ICML*, 2025.

628 34 Jie Lu, Jiaqi Gao, Fei Feng, Zhiqiang He, Menglei Zheng, Kun Liu, Jun He, Binbin Liao,  
 629 Suwei Xu, Ke Sun, et al. Alibaba Stellar: A new generation RDMA network for cloud AI. In  
 630 *ACM SIGCOMM*, pages 453–466, 2025.

631 35 Saf Malik. Zuckerberg: Meta to spend 'hundreds of billions' on AI data centres for superintelligence  
 632 push . <https://www.capacitymedia.com/article-zuckerberg-meta-ai-data-centres>, 2025.

634 36 Sarah McClure, Sylvia Ratnasamy, and Scott Shenker. Load balancing for AI training  
 635 workloads. *arXiv preprint arXiv:2507.21372*, 2025.

636 37 Behnam Montazeri, Yilong Li, Mohammad Alizadeh, and John Ousterhout. Homa: A receiver-  
 637 driven low-latency transport protocol using network priorities. In *ACM SIGCOMM*, pages  
 638 221–235, 2018.

639 38 Yang Nie, Zheng Shi, Xinyi Chen, and Liguo Qian. An out-of-order packet processing algorithm  
 640 of RoCE based on improved SACK. In *IEEE Advanced Information Technology, Electronic  
 641 and Automation Control Conference (IAEAC)*, pages 1402–1408, 2022.

642 39 NVIDIA. NVIDIA InfiniBand Adaptive Routing Technology Accelerating HPC and AI  
 643 Applications. [https://www.amax.com/content/files/2023/12/NVIDIA\\_InfiniBand\\_Adaptive\\_Routing\\_Technology\\_Insights\\_Whitepaper.pdf](https://www.amax.com/content/files/2023/12/NVIDIA_InfiniBand_Adaptive_Routing_Technology_Insights_Whitepaper.pdf), 2023.

645 40 NVIDIA. Connectx-8 supernic datasheet. <https://nvdam.widen.net/s/pxsjzhgw6j/connectx-datasheet-connectx-8-supernic-3231505>, 2024. Datasheet.

647 41 NVIDIA. NVIDIA Spectrum-X Network Platform Architecture. <https://resources.nvidia.com/en-us-networking-ai/nvidia-spectrum-x>, 2024.

649 42 Vladimir Olteanu, Haggai Eran, Dragos Dumitrescu, Adrian Popa, Cristi Baciu, Mark Sil-  
 650 berstein, Georgios Nikolaidis, Mark Handley, and Costin Raiciu. An edge-queued datagram  
 651 service for all datacenter traffic. In *Usenix NSDI*, pages 761–777, 2022.

652 43 OpenAI. Stargate advances with 4.5 GW partnership with Oracle. <https://openai.com/index/stargate-advances-with-partnership-with-oracle/>, 2025.

654 44 PA Governor's Press Office. Governor Josh Shapiro Announces Amazon Plans to Invest \$20  
 655 Billion in Pennsylvania for AI Infrastructure. <https://dced.pa.gov/newsroom/governor-josh-shapiro-announces-amazon-plans-to-invest-20-billion-in-pennsylvania-for-a-i-infrastructure-in-largest-capital-investment-in-commonwealth-history/>, 2025.

658 45 Dylan Patel, Daniel Nishball, and Jeremie Eliahou Ontiveros. Multi-Datacenter Training:  
 659 OpenAI's Ambitious Plan To Beat Google's Infrastructure. <https://semanalysis.com/2024/09/04/multi-datacenter-training-openais/>, 2024.

661 46 Chenchen Qi, Wenfei Wu, Yongcan Wang, Keqiang He, Yu-Hsiang Kao, Zongying He, Chen-Yu  
 662 Yen, Zhuo Jiang, Feng Luo, Surendra Anubolu, et al. SGLB: Scalable and robust global load  
 663 balancing in commodity AI clusters. In *ACM SIGCOMM*, pages 626–644, 2025.

664 47 Kun Qian, Yongqing Xi, Jiamin Cao, Jiaqi Gao, Yichi Xu, Yu Guan, Binzhang Fu, Xuemei  
 665 Shi, Fangbo Zhu, Rui Miao, et al. Alibaba HPN: A data center network for large language  
 666 model training. In *ACM SIGCOMM*, pages 691–706, 2024.

667 48 Costin Raiciu and Gianni Antichi. NDP: Rethinking datacenter networks and stacks two years  
 668 after. *ACM SIGCOMM Computer Communication Review*, 49(5):112–114, 2019.

669 49 Sudarsanan Rajasekaran, Manya Ghobadi, and Aditya Akella. CASSINI: Network-aware job  
 670 scheduling in machine learning clusters. In *Usenix NSDI*, pages 1403–1420, 2024.

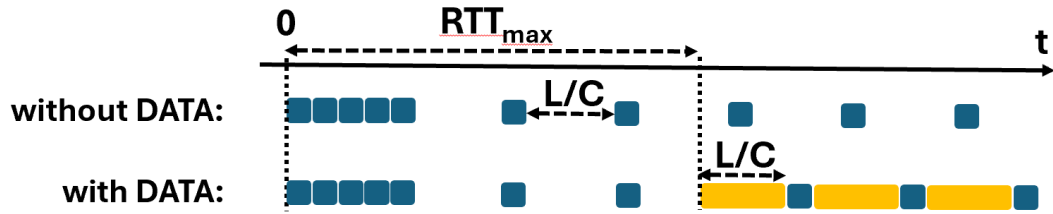


Figure 14 DCsim token-bucket example

671 50 Peter Rizk. Turbocharging Generative AI Workloads with NVIDIA Spectrum-X Networking  
672 Platform. [https://developer.nvidia.com/blog/turbocharging-ai-workloads-with-nvi](https://developer.nvidia.com/blog/turbocharging-ai-workloads-with-nvidia-spectrum-x-networking-platform/)  
673 dia-spectrum-x-networking-platform/, 2023.

674 51 Chenchen Shou, Guyue Liu, Hao Nie, Huaiyu Meng, Yu Zhou, Yimin Jiang, Wenqing Lv,  
675 Yelong Xu, Yuanwei Lu, Zhang Chen, et al. InfiniteHBD: Building datacenter-scale high-  
676 bandwidth domain for LLM with optical circuit switching transceivers. In *ACM SIGCOMM*,  
677 pages 1–23, 2025.

678 52 Cha Hwan Song, Xin Zhe Khooi, Raj Joshi, Inho Choi, Jialin Li, and Mun Choon Chan.  
679 Network load balancing with in-network reordering support for rdma. In *ACM SIGCOMM*,  
680 pages 816–831, 2023.

681 53 Dan Straussman et al. dcSim repository. <https://github.com/danstr1/dcsim>, 2025.

682 54 Lide Suo, Yiren Pang, Wenxin Li, Renjie Pei, Keqiu Li, Xiulong Liu, Xin He, Yitao Hu, and  
683 Guyue Liu. PPT: A pragmatic transport for datacenters. In *ACM SIGCOMM*, pages 954–969,  
684 2024.

685 55 Terabit Ethernet. dcPIM repository. <https://github.com/Terabit-Ethernet/dcPIM>, 2025.

686 56 Ultra Ethernet Consortium. Ultra EthernetTM Specification v1.0. <https://ultraethernet.org/wp-content/uploads/sites/20/2025/06/UE-Specification-6.11.25.pdf>, 2025.

687 57 Moshe Voloshin. Introduction to Congestion Control for RoCE. Technical report, Broadcom  
688 Inc., 2023. URL: "<https://docs.broadcom.com/doc/NCC-WP1XX>".

689 58 Yongji Wu, Yechen Xu, Jingrong Chen, Zhaodong Wang, Ying Zhang, Matthew Lentz, and  
690 Danyang Zhuo. MCCS: A service-based approach to collective communication for multi-tenant  
691 cloud. In *ACM SIGCOMM*, pages 679–690, 2024.

692 59 Jie Zhang, Dafang Zhang, and Kun Huang. Improving datacenter throughput and robustness  
693 with Lazy TCP over packet spraying. *Computer Communications*, 62:23–33, 2015.

## 695 A Proofs

696 **Proof of Theorem 1.** Consider first a case where there are no DATAs, starting from a time  
697  $t = 0$  where many SIMs appear. As illustrated in Fig. 14 (without DATA), the token bucket  
698 first releases a batch of SIMs until it has no more tokens, then releases the following SIMs  
699 periodically as in a simple leaky bucket. These next SIMs are sent every  $\frac{\ell}{C} = \frac{\ell+L}{C}$ , allowing  
700 for the transmission of an  $\ell$ -sized SIM and then for an interpacket gap equivalent to an  
701  $L$ -sized DATA.

702 Now, assume we also get the first DATA  $RTT_{max}$  after the SIM (bottom row of Fig. 14).  
703 The start is the same. However, after  $RTT_{max}$ , a DATA arrives at the DATA queue. It will  
704 be serviced either immediately (if there is no currently serviced SIM) or just as the SIM  
705 departs. Then, when the DATA departs, (a) there is a SIM in the SIM queue by assumption,  
706 and (b) since the DATA lasts  $\frac{L}{C}$  time, at least  $\frac{L+\ell}{C}$  has passed since the last SIM used its  
707 token, so there is also a token for the SIM packet. Thus, a SIM packet is serviced. Since we  
708 assumed that there are always DATA packets in the queue after the first one, it is followed  
709 by a DATA packet. And so on periodically. Since the SIM packet is serviced exactly at the

710 rate of the token bucket, tokens do not accumulate and there is never more than one token  
 711 available between the end of a DATA packet and the start of the next one.

712 As a result, SIMs and DATA are serviced in an *alternating sequence*, and they full occupy  
 713 the line, i.e., *their total rate is  $C$* . ◀

714 **Proof of Theorem 2.** The sum of the time it takes for a SIM to get from  $S$  to  $D$  and the  
 715 time for its corresponding SIM-ACK to get from  $D$  to  $S$ , is equal to the sum of the total  
 716 (1) propagation time, (2) transmission time and (3) queueing time.

717 **1. Propagation time.** The total propagation round-trip time is at most  $RTT_p$ .

718 **2. Transmission time.** The SIM and then the SIM-ACK cross  $2H$  hops. The transmission  
 719 time at each hop is  $\frac{\ell}{C}$ , yielding a total of  $2H \cdot \frac{\ell}{C}$ .

720 **3. Queueing time.** A SIM entering the SIM buffer encounters at most  $B - 1$  SIMs in the  
 721 queue. If it is the first SIM in the queue, it will leave in at most  $\frac{\ell \cdot (\alpha + 2.1)}{C} + \frac{L}{C}$ , where the first  
 722 term accounts for the maximum time it takes for the token bucket to allow departure, and  
 723 the second term accounts for the maximum time a non-SIM packet may block the SIM packet  
 724 (non-preemption), following Equation (2). Since it finds up to  $B - 1$  SIMs in the queue upon  
 725 arrival, it will leave in at most  $\frac{B \cdot \ell \cdot (\alpha + 2.1)}{C} + \frac{L}{C}$ . Accounting for  $2H$  hops and using  $L = \alpha \cdot \ell$ ,  
 726 we get an upper bound of  $2H \cdot \frac{(B+1) \cdot \alpha \cdot \ell + 2.1B \cdot \ell}{C}$ .

727 Finally, after summing all three terms,

$$728 \quad RTT_{\max} = RTT_p + \frac{2H \cdot \ell}{C} \cdot ((B + 1) \cdot \alpha + 2.1B + 1) \quad (7)$$

729 ◀

730 **Proof of Theorem 3.** (i) First, let's explain why a token bucket of size 1 does not work.  
 731 We saw that SIMs can be delayed by at most  $T = \frac{L}{C}$  time when a lower-priority DATA is  
 732 currently being transmitted. When using a bucket of size 1, it may set a worst-case pattern  
 733 where after each SIM is sent, the next SIM (1) first waits for the token-bucket gap time of  
 734  $T' = \frac{\ell}{\frac{C}{\alpha+2.1}} = \frac{L+2.1\ell}{C}$  (using  $L = \alpha \cdot \ell$ ); (2) then whenever this next SIM is ready to receive the  
 735 token, a DATA just starts transmission and delays it for another  $T$ . Thus, the time between  
 736 two SIMs will be up to  $T + T'$ , yielding only about half the needed line rate.

737 (ii) If the token bucket size is 2, assume that at least one SIM is in the SIM queue. Then  
 738 while a first SIM may wait for some DATA transmission to complete and then expects to  
 739 receive its token, the token for the next SIM can still keep coming. Note that  $T' = \frac{L+2.1\ell}{C} >$   
 740  $\frac{L+\ell}{C} = T + \frac{\ell}{C}$ . Thus, after the first SIM departs, the second one will not have received its  
 741 token yet in such a case. Therefore, there is no lack of token for the SIM behind it, proving  
 742 that two tokens are sufficient. In other words, once there are several SIMs in the queue and  
 743 assuming an infinite stream of SIMs, then after an initial period the SIMs will not differentiate  
 744 between two tokens and any higher number, e.g.,  $B \geq 2$ .

745 Note that if the queue is empty, a token bucket of size 2 may lead to a small burst of 2  
 746 SIMs. It is still better than a burst of  $B$  SIMs. Also, if we had a small buffer of one SIM in  
 747 front of the SIM queue and before the arbiter, we could have used a token bucket of size 1,  
 748 or a simple leaky bucket. This is the small cost of relying on a commodity switch. ◀